BIOCHEMISTRY
including biophysical chemistry & molecular biology
Article

Biochemistry **2009,** *48,* 7533–7538 7533
DOI: 10.1021/bi900669m

Impact of Actin Glutathionylation on the Actomyosin-S1 ATPase†

Gresin O. Pizarro and Ozgur Ogut*

Division of Cardiovascular Diseases, Mayo Clinic, Rochester, Minnesota 55902

Received April 19, 2009; Revised Manuscript Received July 2, 2009

ABSTRACT: Glutathionylation of intracellular proteins is an established physiological regulator of protein function. In multiple models, including ischemia-reperfusion of the heart, increased oxidative stress results in the glutathionylation of sarcomeric actin. We hypothesized that actin glutathionylation may play a role in the multifactorial change in cardiac muscle contractility observed during this pathophysiological state. Therefore, the functional impact of glutathionylated actin on the interaction with myosin-S1 was examined. Substituting glutathionylated F-actin for unmodified F-actin reduced the maximum actomyosin-S1 ATPase, and this was accompanied by an increase in the activation energy of the steady state ATPase. Measurement of steady state binding did not suggest a large impact of actin glutathionylation on the binding to myosin-S1. However, transient binding and dissociation kinetics determined by stopped-flow methods demonstrated that although actin glutathionylation did not significantly alter the rate constant of myosin-S1 binding, there was a significant decrease in the rate of ATP-induced myosin-S1 detachment in the presence of ADP. These results suggest that actin glutathionylation may play a limited but defined role in the alteration of contractility following oxidative stress to the myocardium, particularly through a decrease in the actomyosin ATPase activity.

Oxidative modification of proteins has been shown to have a significant impact on the function of multiple biological systems (*1*), and protein glutathionylation in response to oxidative stress has thereby emerged as a novel method for regulating protein function (*2*−*4*). The glutathionylation of actin in response to oxidative stress has been observed in the myocardium following ischemia-reperfusion, complementing similar observations in lymphocytes and fibroblasts (*4*−*7*). Previous studies have demonstrated that the glutathionylation of actin occurs reversibly at Cys374 (*4*, *5*), and the functional impact of this post-translational modification may range from a reduction in the time course and extent of actin polymerization to altered signaling during integrin-mediated cell adhesion (*4*, *5*, *8*). For cells that depend on the reorganization of the F-actin[1] network for motility, the impact of glutathionylation on F-actin polymerization provides a reliable corollary to functional impact. However, for nonmotile cells such as cardiomyocytes, the functional consequence of actin glutathionylation remains unclear. Under physiological conditions, actin serves as the important binding partner for myosin in the actomyosin cross-bridge cycle (*9*), and the regulation of this interaction is intimately linked to optimal force production. However, under pathophysiological conditions that reduce myocardial blood flow to the heart, the resultant decrease in contractility may be related to reversible post-translational modification of myofilament proteins (*10*−*13*). Therefore, actin's vital role in force generation in cardiomyocytes may implicate glutathionylation as a reversible post-translational modification that is a physiologically meaningful contributor to altered contractility (*9*).

To deconstruct the impact of actin glutathionylation in cardiac muscles, we tested in vitro glutathionylated actin for its ability to support the actomyosin-S1 ATPase, as well as its steady state and transient binding properties with myosin-S1. Although there was no change in the steady state binding of actin to myosin-S1, the actin-activated myosin-S1 ATPase was reduced when glutathionylated F-actin was used as compared to unmodified F-actin. Stopped-flow analyses of transient binding kinetics suggested that this outcome was related to slower ATP-induced dissociation of glutathionylated actomyosin-S1 in the presence of ADP. These data provide initial insight into the functional consequences of actin glutathionylation in the myocardium.

MATERIALS AND METHODS

Protein Preparation. G-Actin was prepared from rabbit skeletal muscle acetone powder (Pel-freez) on the basis of a published method (*14*). The protocol was followed as described, save for the substitution of 2 mM PIPES (pH 7) for 2 mM Tris-HCl (pH 8) during the purification procedure. The purified G-actin was glutathionylated as previously described (*8*, *12*, *15*). Briefly, G-actin (∼80 μM) was incubated with a 10-fold molar excess of DTNB dissolved in 0.12 M $NaHCO_3$. The reaction was terminated by gel filtration using Sephadex G25 (GE Healthcare). The concentration of the gel-filtered G-actin was determined by A_{290} (E = 26460 M^{-1} cm^{-1}), and a 20-fold molar excess of glutathione dissolved in 50 mM PIPES (pH 7) was added. The reaction was followed at A_{412} for the net release of TNB^- (E = 14150 M^{-1} cm^{-1}), which was equal to the concentration of glutathionylated G-actin. This concentration, divided by the total concentration of G-actin in the reaction mixture, gave the percentage of glutathionylated G-actin. Free

†This work was supported by National Institutes of Health Grant R01 HL78845 to O.O.

*To whom correspondence should be addressed: Division of Cardiovascular Diseases, Mayo Clinic, 200 First St, S.W., Rochester, MN 55902. E-mail: ogut.ozgur@mayo.edu. Phone: (507) 538-8196. Fax: (507) 538-6418.

[1]Abbreviations: AM, actomyosin; DTT, dithiothreitol; F-actin, filamentous actin; G-actin, globular actin.

Published on Web 07/06/2009

glutathione and TNB^- were removed from the G-actin by gel filtration as described above, and the concentration of G-actin was again measured. Typically, 65−70% of the G-actin was glutathionylated using this procedure. To prepare mixtures of 20 and 40% glutathionylated actin, unmodified G-actin was added to the appropriate amount to yield the desired final glutathionylation percentage. G-Actin was polymerized into F-actin by two rounds of dialysis against 2 L of 50 mM KCl, 10 mM BES (pH 7), 4 mM $MgCl_2$, and 1 mM EGTA (*16*). Each preparation of polymerized F-actin was used for only 1 day. To independently confirm actin glutathionylation, Western blotting was conducted with an anti-glutathione monoclonal antibody (Virogen) as previously described (*12*). Detection was achieved with ECL Plus substrate scanned for fluorescence on a Typhoon 9410 scanner (GE Lifesciences).

Myosin was prepared from porcine hearts according to a previously described method (*17*). To prepare myosin-S1, the myosin was dialyzed against 0.12 M NaCl, 1 mM EDTA, and 20 mM sodium phosphate buffer (pH 7) and digested at 4 °C for 4 h with a ratio of 3.3 mg of chymotrypsin for every gram of myosin. The reaction was terminated by the addition of diisopropyl fluorophosphate to a final concentration of 12 mM, and the myosin-S1 was separated by centrifugation at 125000*g* for 2 h.

Steady State Actomyosin Binding and ATPase. To measure the impact of actin glutathionylation on the steady state interaction of actin and myosin-S1, binding was assessed by a light scattering method (*16*). F-Actin prepared from unmodified or glutathionylated G-actin was added to a final concentration of 0.6 μM to a buffer containing 100 mM KCl, 10 mM BES (pH 7), 4 mM $MgCl_2$, and 1 mM EGTA. This solution was mixed in a 1.5 mL quartz cuvette (Hellma) with a micro stir bar and monitored with a Shimadzu RF-5301 PC spectrofluorometer for light scattering using 340 nm incident light. The cuvette holder was jacketed with circulating water to maintain a temperature of 25 °C. To the F-actin mixture was added myosin-S1, and the increase in light scattering was measured. At all concentrations of myosin-S1 tested, the added volume of myosin-S1 was less than 1% of the total reaction volume. To dissociate the actomyosin-S1, ATP was added to a final concentration of 40 μM. The difference in light scattering before and after ATP addition was representative of myosin-S1 binding to actin (*16*). Results are presented as averages ± the standard error of the mean (SEM).

The level of steady state actomyosin ATPase was measured on the basis of a linked assay as described previously (*18*, *19*). Varying concentrations of polymerized actin were mixed in a buffer containing 25 mM KCl, 10 mM BES (pH 7), 4 mM $MgCl_2$, and 1 mM EGTA that included 40 units/mL lactate dehydrogenase, 200 units/mL pyruvate kinase, and 500 nM myosin-S1 and allowed to equilibrate for 5 min. The ATPase reaction was initiated by the addition of a substrate mix to bring the final concentrations of ATP (Special grade, Roche), phosphoenolpyruvate, and NADH to 2, 0.5, and 0.2 mM, respectively. The reaction was followed by A_{340}, which represented the oxidation of NADH in response to production of ADP from actomyosin-S1. Slopes of the change in absorbance over time were converted to a rate of ATP consumed per second per myosin head and plotted versus actin concentration. Each data set was fit individually as described previously (*20*), and the parameters from the individual fits were then averaged. The activation energy was measured by determining the net steady state ATPase level of 500 nM myosin-S1 in the presence of 35 μM F-actin at 10, 15, 20, and 25 °C. The Arrhenius plots were used to determine the slope of the relationship between ln(rate) and 1/temperature (K^{-1}), which gave the activation energy divided by the gas constant R (−1.987 cal K^{-1} mol^{-1}).

Stopped-Flow Analyses. The transient binding kinetics of unmodified and glutathionylated F-actin with myosin-S1 were studied by the stopped-flow method using an SF-2001 apparatus (KinTek Corp.). For these experiments, the buffer consisted of 50 mM KCl, 10 mM BES (pH 7), 4 mM $MgCl_2$, and 1 mM EGTA. To assess the binding of myosin-S1 to F-actin, one syringe was filled with 2 μM polymerized F-actin and the other syringe was filled with varying concentrations of myosin-S1 that were treated for 5 min with 0.01 unit of apyrase. Syringe contents were mixed by the stopped-flow method, and binding was followed by light scattering at 340 nm. All experiments were performed at 15 °C. Typically, six to eight records were averaged to determine the binding profile at a given concentration. The averaged actomyosin binding profile was fit to a single exponential to determine the rate of binding at each myosin-S1 concentration.

To determine the rates of dissociation of actomyosin-S1 by ATP, one syringe was filled with a mixture of 4 μM F-actin and 3.5 μM myosin-S1 in the presence of 0.01 unit of apyrase and allowed to incubate at 15 °C for 5 min. The actomyosin was dissociated by stopped-flow mixing with varying concentrations of ATP up to 0.5 mM. The profile of the dissociation was fit by a single exponential to determine the observed first-order rate constant at each nucleotide concentration. In the absence of ADP, attempts to measure rates of detachment at > 0.5 mM ATP were not reliable as a significant magnitude of the detachment occurred during the dead time of the instrument (*21*). For experiments testing the effect of 12.5 μM ADP on the rate of detachment, the actomyosin-S1 syringe did not include apyrase but included ADP and 5 μM diadenosine pentaphosphate (*16*).

RESULTS

Steady State Binding of Glutathionylated F-Actin with Myosin-S1. G-Actin was glutathionylated using previously published methods (*8*, *12*, *15*). The efficacy of the glutathionylation procedure is demonstrated in Figure 1. As expected, the anti-glutathione antibody did not identify unmodified G-actin, but the glutathionylated actins were readily labeled in a manner proportional to the extent of modification. The identification of glutathionylated actin by the anti-glutathione antibody was not a result of nonspecific labeling, as reversal of glutathionylation by DTT abrogated the antibody signal. Using the unmodified and glutathionylated F-actin preparations, the steady state binding of porcine myosin-S1 to F-actin was assessed by light scattering (Figure 2). As previously demonstrated, the binding demonstrates a linear increase followed by a sharp plateau (*16*). All three relationships were superimposable over the linear phase, suggesting no change in the association constant. Furthermore, the magnitudes of the light scattering at the plateau for normal and glutathionylated actins were not different, suggesting no change in the stoichiometry of binding.

Actomyosin ATPase with Glutathionylated F-Actin. The impact of actin glutathionylation on the steady state actin-activated ATPase of myosin-S1 was measured at 25 °C by tracking ATP consumption indirectly through oxidation of NADH by a linked enzymatic assay (*18*, *19*). Although the ATPase of porcine myosin-S1 mixed with unmodified F-actin demonstrated activity

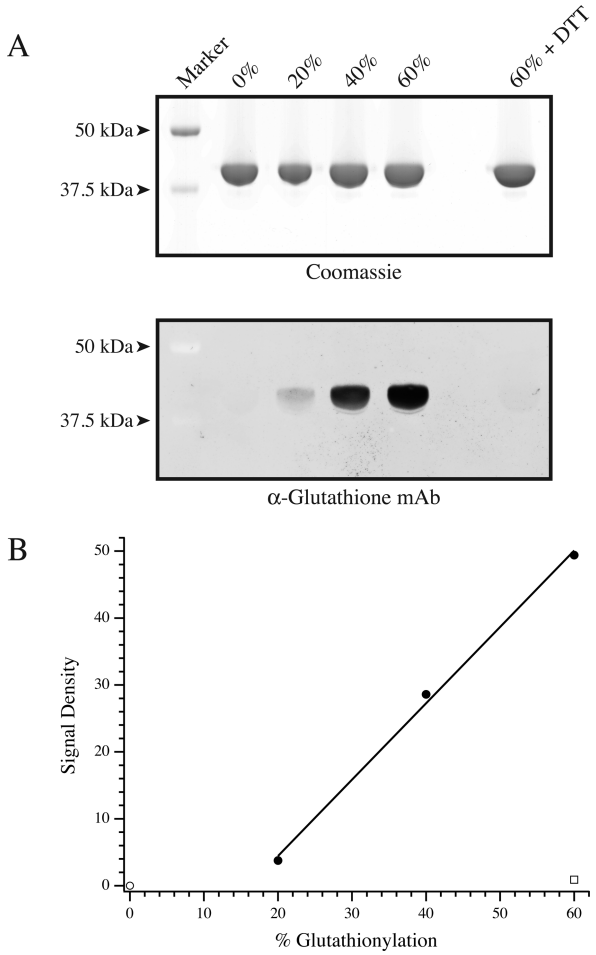

FIGURE 1: Glutathionylation of G-actin. (A) In the top panel, aliquots of unmodified and 20, 40, and 60% glutathionylated G-actin, along with 60% glutathionylated G-actin treated with DTT, were resolved by SDS−PAGE and stained by Coomassie blue. In the bottom panel, a duplicate gel was transferred and Western blotted with an anti-glutathione monoclonal antibody to identify glutathionylated vs unmodified G-actin. (B) Following densitometry, the anti-glutathione Western blot signal was divided by the total actin signal to determine the signal density (arbitrary units) of glutathionylation. The graph denotes unmodified G-actin (○), plotted with G-actins glutathionylated to 20, 40, and 60% (●) as well as 60% glutathionylated G-actin that was treated with DTT prior to Western blotting (□).

on par with previously published results (*21*, *22*), the V_{max} of myosin-S1 was significantly reduced when F-actin was polymerized from 20 or 40% glutathionylated G-actin (Figure 3A). The measured V_{max} was 0.56 ± 0.08 ATP s^{-1} $head^{-1}$ (n = 7) for unmodified F-actin but saw statistically significant declines to 0.33 ± 0.07 (n = 4) and 0.24 ± 0.08 ATP s^{-1} $head^{-1}$ (n = 3) with 20 and 40% glutathionylated F-actin, respectively. This was accompanied by a decrease in the concentration of actin required for half-maximal activity from 18.6 ± 3.0 μM for unmodified F-actin to 10.0 ± 1.9 and 9.3 ± 1.0 μM for 20 and 40% glutathionylated F-actin, respectively. The activation energy of the ATPase was measured for unmodified and 40% glutathionylated F-actin and was 18.4 ± 0.6 kcal/mol (n = 4) for unmodified F-actin and rose significantly to 29.3 ± 4.8 kcal/mol (n = 3) for 40% glutathionylated F-actin (Figure 3B; $P < 0.05$).

Stopped-Flow Analyses of Actomyosin Interaction. To complement the steady state analyses, stopped-flow experiments

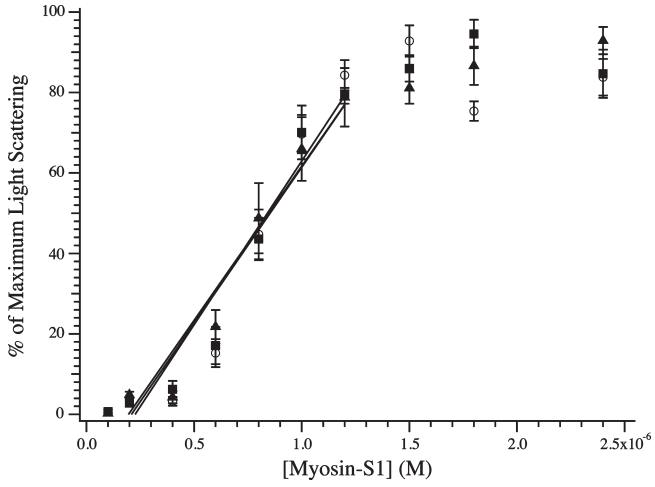

FIGURE 2: Steady state binding of myosin-S1 to F-actin. The binding of myosin-S1 to unmodified (○), 20% glutathionylated (■), or 40% glutathionylated (▲) F-actin (600 nM each) was assessed by light scattering at 340 nm. The data are plotted as a percentage of maximum light scattering. The presence of glutathionylated actin did not impact the binding of myosin-S1 during the linear phase (represented by linear fits), nor was there a difference in the absolute magnitude of light scattering at the plateau (data not shown).

were undertaken to determine transient binding and dissociation kinetics of glutathionylated F-actin with myosin-S1. The second-order rate constant of binding for porcine myosin-S1 to unmodified F-actin was (1.6 ± 0.1) × 10^6 M^{-1} s^{-1} (n = 2), which was similar to previously published data for cardiac muscle myosin-S1 (*16*). There was not a significant change in the rate constant for binding of myosin-S1 to 20% glutathionylated F-actin, which was (1.4 ± 0.3) × 10^6 M^{-1} s^{-1} (n = 2).

The rates of actomyosin-S1 or actomyosin-S1·ADP dissociation by ATP were measured on the basis of previously established methods (*16*, *21*). Titration of ATP resulted in an increase in the observed rates of dissociation of myosin-S1 from F-actin (Figure 4), modeled as the second and third steps of the following scheme (*21*,*23*,*24*):

$$\mathrm{AM{\cdot}ADP} \underset{k_{-1}}{\overset{k_1}{\rightleftarrows}} \mathrm{AM} + \mathrm{ATP} \underset{k_{-1}}{\overset{k_1}{\rightleftarrows}} \mathrm{AM{\cdot}ATP} \underset{k_{-2}}{\overset{k_2}{\rightleftarrows}} \mathrm{A} + \mathrm{M{\cdot}ATP}$$

Accordingly, the observed rates of dissociation of myosin-S1 were measured for up to 0.5 mM ATP and were fit to the equation $k_{obs} = k_2[K_1[ATP]/(K_1[ATP]+1)]$. Best fits of the data provided apparent second-order rate constants (K_1k_2) of (2.4 ± 0.7) × 10^6 M^{-1} s^{-1} for unmodified F-actin and (2.5 ± 0.4) × 10^6 and (2.4 ± 0.5) × 10^6 M^{-1} s^{-1} for 20 and 40% glutathionylated F-actin, respectively. The rates, k_2, representing the maximum rates of actomyosin-S1 dissociation by ATP were estimated to be 1702 ± 293, 1299 ± 359, and 1319 ± 357 s^{-1} when using 0, 20, and 40% glutathionylated F-actin, respectively. At high ATP concentrations, dissociation rates approach 2000 s^{-1} and detachment occurs primarily during the dead time of the stopped-flow instrument (*16*, *17*, *21*), suggesting that these values should be derived with caution. The kinetics of dissociation for ADP-free actomyosin-S1 by ATP were complemented by measuring the ATP-dependent dissociation of actomyosin-S1 in the presence of 12.5 μM ADP (Figure 5). For unmodified F-actin, the rate reached a plateau at 46.6 ± 2.7 s^{-1} (n = 4), which was in line with prior published results (*16*). This rate was significantly reduced to 31.8 ± 3.8 s^{-1}

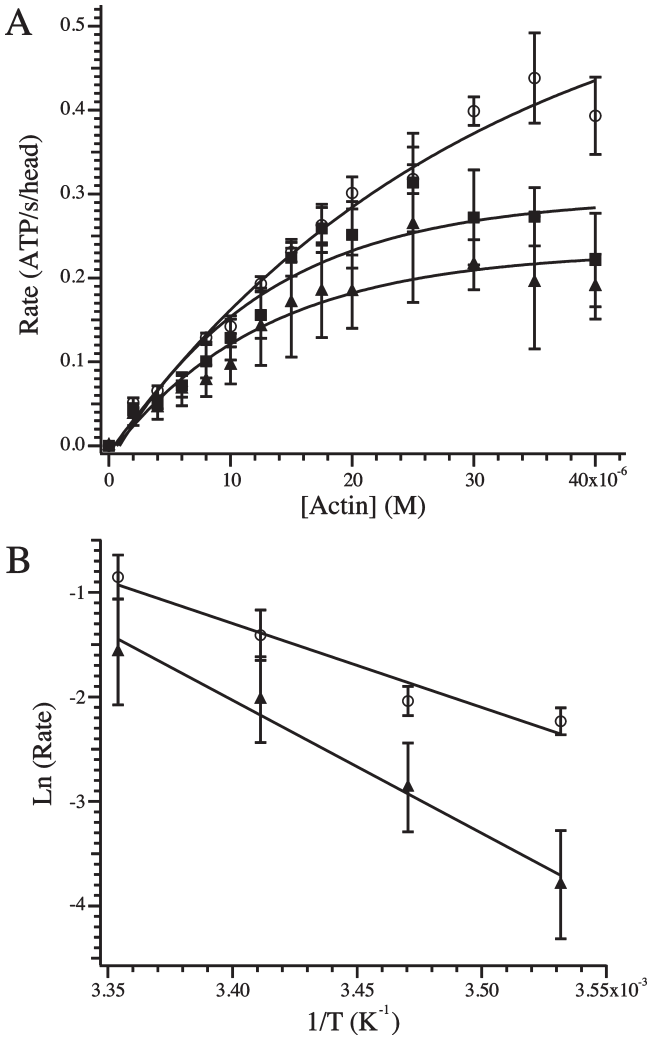

FIGURE 3: Actomyosin ATPase and activation energy. (A) Rates of actomyosin-S1 ATPase using unmodified (○) and 20 (■) and 40% (▲) glutathionylated F-actin. The concentration of F-actin required for half-maximal activity was 18.6 ± 3.0 μM for unmodified F-actin vs 10.0 ± 1.9 and 9.3 ± 1.0 μM for 20 and 40% glutathionylated F-actin, respectively. The maximum rates were 0.56 ± 0.08, 0.33 ± 0.07, and 0.24 ± 0.08 ATP s^{-1} head^{-1} for unmodified and 20 and 40% glutathionylated F-actin, respectively. Exponential fits to the averaged data are shown for illustrative purposes. (B) The activation energy of the ATPase reaction was measured for unmodified and 40% glutathionylated F-actin by plotting ln(rate) vs the reciprocal of the temperature (in kelvin). The activation energies calculated from the slopes were 18.4 ± 0.6 kcal/mol for unmodified F-actin and 29.3 ± 4.8 kcal/mol for 40% glutathionylated F-actin.

($n = 3$) and 30.9 ± 2.1 s^{-1} ($n = 3$) for 20 and 40% glutathionylated F-actin, respectively ($P < 0.05$).

DISCUSSION

Oxidative modification of proteins in response to cellular stress is a recognized route of functional regulation (*1*). Multiple models have demonstrated that isoforms of actin may be glutathionylated in response to oxidative stress, implicating this as an important and fundamental regulatory mechanism (*4*−*6*). The functional impact of actin glutathionylation has been primarily measured as a reduction in the extent of polymerization of glutathionylated G-actin into F-actin (*5*, *25*), although recent evidence has shown that it may alter integrin-mediated signaling during cell adhesion (*4*). For motile cells that require rapid reorganization of the F-actin network, glutathionylation would therefore represent an intuitive mechanism of functional regulation that is readily reversible. However, actin in the cardiomyocytes is the backbone of the thin filament of the sarcomere and does not rely on polymerization−depolymerization cycles to support contraction through cross-bridge cycling with myosin. Therefore, to better define the functional impact that actin

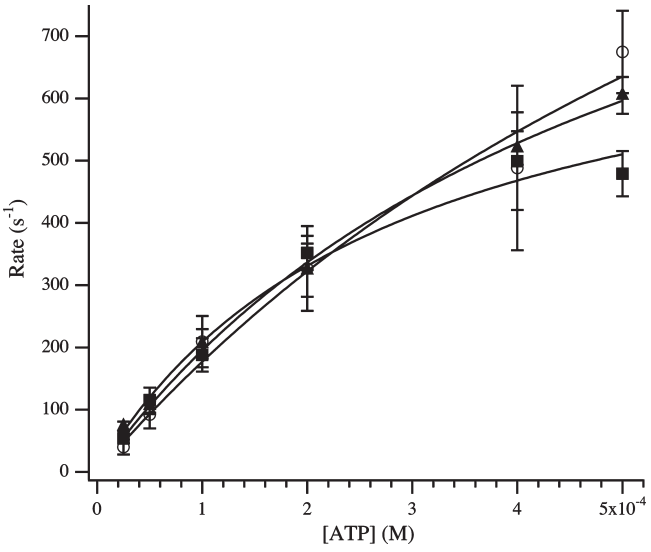

FIGURE 4: Dissociation of actomyosin-S1 by ATP. Unmodified or glutathionylated F-actin (4 μM) was incubated with myosin-S1 (3.5 μM) to form actomyosin-S1. The bound complex was dissociated by stopped-flow mixing with varying concentrations of ATP. The rate of the exponential decline in light scattering was plotted as a function of ATP and fit by a modified equation (see Materials and Methods). Approximate values of the maximum rate of ATP-induced dissociation were 1702 ± 293, 1299 ± 359, and 1319 ± 357 s^{-1} for unmodified (○), 20% glutathionylated (■), and 40% glutathionylated (▲) F-actin, respectively.

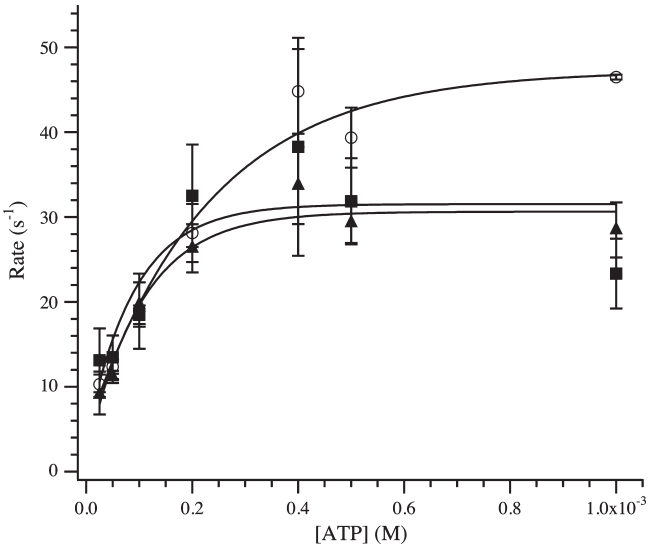

FIGURE 5: Dissociation of actomyosin-S1·ADP by ATP. Unmodified or glutathionylated F-actin (4 μM) was mixed with myosin-S1 (3.5 μM) in the presence of 25 μM ADP to form actomyosin-S1·ADP. This complex was dissociated by varying concentrations of ATP, and these rates were plotted to determine the rate of dissociation of ADP from the actomyosin-S1 complex. For unmodified F-actin (○), the maximum rate of ATP-induced dissociation was 46.6 ± 2.7 s^{-1}, significantly higher than those for 20% [31.8 ± 3.8 s^{-1} (■)] and 40% [30.9 ± 2.1 s^{-1} (▲)] glutathionylated F-actin.

glutathionylation may have in cardiac muscle, we examined its effect on the actin-activated myosin-S1 ATPase as well as steady state and transient myosin-S1 binding properties.

Most significantly, we observed that F-actin polymerized from glutathionylated G-actin demonstrated lower maximum rates of actin-activated myosin-S1 ATPase activity (Figure 3). These data suggest that in situ glutathionylation of actin monomers in the thin filament during ischemia-reperfusion of the heart may be a factor contributing to the observed decrease in the maximum force production by permeabilized fibers from these hearts (*12*). The reduction in the maximum rate of ATPase may generally have been due to reduced total myosin-S1 attachment or slowed myosin-S1 detachment (*26*). A difference in attachment appeared unlikely, as the steady state association of myosin-S1 with actin was unchanged when using glutathionylated actin, nor was there a change in the apparent stoichiometry of binding. These observations were complemented by stopped-flow studies to determine the possible transient kinetic differences in select transitions of the cross-bridge cycle. Measurements of the second-order rate constant for myosin-S1 binding to F-actin were not influenced by glutathionylation, which was generally unsurprising given the steady state binding data. Therefore, it was unlikely that the transitions governing initial association of myosin-S1 with glutathionylated F-actin were the catalysts for reduced ATPase activity. This prompted the examination of cross-bridge transitions that defined the dissociation of bound actomyosin-S1 complexes. The second-order rates of dissociation of unmodified and glutathionylated actomyosin-S1 triggered by mixing with ATP were not different (Figure 4). However, a significant decrease in the maximum rate of actomyosin-S1·ADP dissociation by ATP was observed. Previous studies have demonstrated that the rate of cross-bridge detachment is a determining factor for the unloaded shortening velocity (*27*). This is a reasonable corollary to the actomyosin-S1 ATPase in solution, as the measurement is taken under effectively unloaded conditions. Furthermore, dissociation of ADP from actomyosin is sufficiently slow to be a controlling step of the ATPase (*26*, *28*), suggesting that conditions mimicking in vivo ADP concentrations may lead to the best assessment of physiological impact. When examining this cross-bridge step, we used a concentration of ADP that would not fully saturate the available actomyosin-S1 sites in an effort to improve our understanding of physiological and pathophysiological conditions where full ADP saturation is unlikely (*29*). Therefore, the reduction in the measured rate of myosin-S1 detachment in the presence of ADP may be a strong contributor to the observed decline in the maximum rate of actomyosin-S1 ATPase in the presence of glutathionylated F-actin and may be a factor in the decreased force production observed in ischemic fibers.

At this point, the mechanism behind actin glutathionylation's effect on the dissociation of the actomyosin-S1·ADP complex is unclear. It is well established that the glutathionylation of G-actin reduces the rate of F-actin formation (*5*, *25*). Furthermore, we had previously demonstrated that the glutathionylation of F-actin leads to a reduction in the cooperativity of tropomyosin binding (*12*). Coupled with the altered rate of actomyosin-S1·ADP dissociation by ATP, these findings may generally suggest that the root cause of the functional impact of actin glutathionylation is a modulation of the intermonomer interactions between adjacent actins along the thin filament. It has been previously demonstrated that myosin-S1 binding to the external surface of the actin filament causes an alteration in the environment of the filament interior (*30*). This is in general agreement with data demonstrating that the actin filament has internal cooperativity, which would aid in propagation of intermonomer interactions (*31*). In fact, these dynamic properties of the actin filament may play unique roles in the contractile process (*32*). We hypothesize that the glutathionylation of actin may impair, to an extent, the internal cooperativity of the actin filament, causing subtle changes in the manner by which thin filament (tropomyosin) or thick filament (myosin-S1) proteins interact with the actin filament. In relation to our current studies, it is therefore possible that the glutathionylation of actin may lead to changes in the intermonomer properties of the actin filament that may inadvertently stabilize the ADP-bound conformation of myosin-S1, thereby reducing eventual cross-bridge detachment.

In conclusion, we provide data to support the role of actin glutathionylation in modulating the actomyosin-S1 ATPase. The presence of glutathionylated actin in ischemia-reperfused hearts may suggest that this post-translational modification contributes to the transient reduction in contractility experienced during altered myocardial blood flow (*12*). However, this pathophysiological condition presents with multiple changes to the contractile filaments, including altered troponin I and myosin binding protein C phosphorylation (*10*, *12*, *13*, *33*, *34*). Therefore, future studies examining the interplay between the various post-translational modifications, especially in the context of the regulated thin filament, will be necessary to define the net impact of actin glutathionylation on contractility.

ACKNOWLEDGMENT

We thank Dr. Frank Brozovich for discussions and critical reading of the manuscript.

REFERENCES

1. Berlett, B. S., and Stadtman, E. R. (1997) Protein oxidation in aging, disease, and oxidative stress. *J. Biol. Chem. 272*, 20313–20316.
2. Sparaco, M., Gaeta, L. M., Tozzi, G., Bertini, E., Pastore, A., Simonati, A., Santorelli, F. M., and Piemonte, F. (2006) Protein glutathionylation in human central nervous system: Potential role in redox regulation of neuronal defense against free radicals. *J. Neurosci. Res. 83*, 256–263.
3. Applegate, M. A., Humphries, K. M., and Szweda, L. I. (2008) Reversible inhibition of α-ketoglutarate dehydrogenase by hydrogen peroxide: Glutathionylation and protection of lipoic acid. *Biochemistry 47*, 473–478.
4. Fiaschi, T., Cozzi, G., Raugei, G., Formigli, L., Ramponi, G., and Chiarugi, P. (2006) Redox regulation of β-actin during integrin-mediated cell adhesion. *J. Biol. Chem. 281*, 22983–22991.
5. Wang, J., Boja, E. S., Tan, W., Tekle, E., Fales, H. M., English, S., Mieyal, J. J., and Chock, P. B. (2001) Reversible glutathionylation regulates actin polymerization in A431 cells. *J. Biol. Chem. 276*, 47763–47766.
6. Fratelli, M., Demol, H., Puype, M., Casagrande, S., Eberini, I., Salmona, M., Bonetto, V., Mengozzi, M., Duffieux, F., Miclet, E., Bachi, A., Vandekerckhove, J., Gianazza, E., and Ghezzi, P. (2002) Identification by redox proteomics of glutathionylated proteins in oxidatively stressed human T lymphocytes. *Proc. Natl. Acad. Sci. U.S.A. 99*, 3505–3510.
7. Pastore, A., Tozzi, G., Gaeta, L. M., Bertini, E., Serafini, V., Di Cesare, S., Bonetto, V., Casoni, F., Carrozzo, R., Federici, G., and Piemonte, F. (2003) Actin glutathionylation increases in fibroblasts of patients with Friedreich's ataxia: A potential role in the pathogenesis of the disease. *J. Biol. Chem. 278*, 42588–42595.
8. Dalle-Donne, I., Rossi, R., Giustarini, D., Colombo, R., and Milzani, A. (2003) Actin S-glutathionylation: Evidence against a thiol-disulphide exchange mechanism. *Free Radical Biol. Med. 35*, 1185–1193.
9. Gordon, A. M., Homsher, E., and Regnier, M. (2000) Regulation of contraction in striated muscle. *Physiol. Rev. 80*, 853–924.

10. Yuan, C., Guo, Y., Ravi, R., Przyklenk, K., Shilkofski, N., Diez, R., Cole, R. N., and Murphy, A. M. (2006) Myosin binding protein C is differentially phosphorylated upon myocardial stunning in canine and rat hearts: Evidence for novel phosphorylation sites. *Proteomics 6*, 4176–4186.
11. Messer, A. E., Jacques, A. M., and Marston, S. B. (2007) Troponin phosphorylation and regulatory function in human heart muscle: Dephosphorylation of Ser23/24 on troponin I could account for the contractile defect in end-stage heart failure. *J. Mol. Cell. Cardiol. 42*, 247–259.
12. Chen, F. C., and Ogut, O. (2006) Decline of contractility during ischemia-reperfusion injury: Actin glutathionylation and its effect on allosteric interaction with tropomyosin. *Am. J. Physiol. 290*, C719–C727.
13. Belin, R. J., Sumandea, M. P., Kobayashi, T., Walker, L. A., Rundell, V. L., Urboniene, D., Yuzhakova, M., Ruch, S. H., Geenen, D. L., Solaro, R. J., and de Tombe, P. P. (2006) Left ventricular myofilament dysfunction in rat experimental hypertrophy and congestive heart failure. *Am. J. Physiol. 291*, H2344–H2353.
14. Pardee, J. D., and Spudich, J. A. (1982) Purification of muscle actin. *Methods Enzymol. 85* (Part B), 164–181.
15. Drewes, G., and Faulstich, H. (1990) The enhanced ATPase activity of glutathione-substituted actin provides a quantitative approach to filament stabilization. *J. Biol. Chem. 265*, 3017–3021.
16. Siemankowski, R. F., and White, H. D. (1984) Kinetics of the interaction between actin, ADP, and cardiac myosin-S1. *J. Biol. Chem. 259*, 5045–5053.
17. Taylor, R. S., and Weeds, A. G. (1976) The magnesium-ion-dependent adenosine triphosphatase of bovine cardiac myosin and its subfragment-1. *Biochem. J. 159*, 301–315.
18. Furch, M., Geeves, M. A., and Manstein, D. J. (1998) Modulation of actin affinity and actomyosin adenosine triphosphatase by charge changes in the myosin motor domain. *Biochemistry 37*, 6317–6326.
19. De La Cruz, E. M., Sweeney, H. L., and Ostap, E. M. (2000) ADP inhibition of myosin V ATPase activity. *Biophys. J. 79*, 1524–1529.
20. De La Cruz, E. M., and Ostap, E. M. (2009) Kinetic and equilibrium analysis of the myosin ATPase. *Methods Enzymol. 455*, 157–192.
21. Pereira, J. S., Pavlov, D., Nili, M., Greaser, M., Homsher, E., and Moss, R. L. (2001) Kinetic differences in cardiac myosins with identical loop 1 sequences. *J. Biol. Chem. 276*, 4409–4415.
22. Malmqvist, U. P., Aronshtam, A., and Lowey, S. (2004) Cardiac myosin isoforms from different species have unique enzymatic and mechanical properties. *Biochemistry 43*, 15058–15065.
23. Ostap, E. M., and Pollard, T. D. (1996) Biochemical kinetic characterization of the Acanthamoeba myosin-I ATPase. *J. Cell Biol. 132*, 1053–1060.
24. El Mezgueldi, M., Tang, N., Rosenfeld, S. S., and Ostap, E. M. (2002) The kinetic mechanism of Myo1e (human myosin-IC). *J. Biol. Chem. 277*, 21514–21521.
25. Dalle-Donne, I., Giustarini, D., Rossi, R., Colombo, R., and Milzani, A. (2003) Reversible S-glutathionylation of Cys 374 regulates actin filament formation by inducing structural changes in the actin molecule. *Free Radical Biol. Med. 34*, 23–32.
26. Siemankowski, R. F., Wiseman, M. O., and White, H. D. (1985) ADP dissociation from actomyosin subfragment 1 is sufficiently slow to limit the unloaded shortening velocity in vertebrate muscle. *Proc. Natl. Acad. Sci. U.S.A. 82*, 658–662.
27. Ferenczi, M. A., Goldman, Y. E., and Simmons, R. M. (1984) The dependence of force and shortening velocity on substrate concentration in skinned muscle fibres from *Rana temporaria*. *J. Physiol. 350*, 519–543.
28. Martin, H., and Barsotti, R. J. (1994) Relaxation from rigor of skinned trabeculae of the guinea pig induced by laser photolysis of caged ATP. *Biophys. J. 66*, 1115–1128.
29. Bottomley, P. A., and Weiss, R. G. (2001) Noninvasive localized MR quantification of creatine kinase metabolites in normal and infarcted canine myocardium. *Radiology 219*, 411–418.
30. Feng, L., Kim, E., Lee, W. L., Miller, C. J., Kuang, B., Reisler, E., and Rubenstein, P. A. (1997) Fluorescence probing of yeast actin subdomain 3/4 hydrophobic loop 262−274. Actin-actin and actin-myosin interactions in actin filaments. *J. Biol. Chem. 272*, 16829–16837.
31. Orlova, A., Prochniewicz, E., and Egelman, E. H. (1995) Structural dynamics of F-actin: II. Cooperativity in structural transitions. *J. Mol. Biol. 245*, 598–607.
32. Prochniewicz-Nakayama, E., Yanagida, T., and Oosawa, F. (1983) Studies on conformation of F-actin in muscle fibers in the relaxed state, rigor, and during contraction using fluorescent phalloidin. *J. Cell Biol. 97*, 1663–1667.
33. Bito, V., van der Velden, J., Claus, P., Dommke, C., Van Lommel, A., Mortelmans, L., Verbeken, E., Bijnens, B., Stienen, G., and Sipido, K. R. (2007) Reduced force generating capacity in myocytes from chronically ischemic, hibernating myocardium. *Circ. Res. 100*, 229–237.
34. Bowling, N., Walsh, R. A., Song, G., Estridge, T., Sandusky, G. E., Fouts, R. L., Mintze, K., Pickard, T., Roden, R., Bristow, M. R., Sabbah, H. N., Mizrahi, J. L., Gromo, G., King, G. L., and Vlahos, C. J. (1999) Increased protein kinase C activity and expression of Ca^{2+}-sensitive isoforms in the failing human heart. *Circulation 99*, 384–391.